Journal of Applied Informatics and Computing (JAIC)
Vol.10, No.3, June 2026, pp. 2520~2533
e-ISSN: 2548-6861

Multi-LoRa-Based Automatic Drinking Water Transmission System

Sri Indah Rezkika[1*], Andri Ramadhan[2], Adinda Juwita Nasution[3***], Muhammad Fiza Lubis[4****], Panangian Mahadi Sihombing[5*****], Aulia Agung Dermawan[6******]**
* Electrical Engineering, Faculty of Engineering, Al-Azhar University, Indonesia
** Mechanical Engineering, Faculty of Engineering, Al-Azhar University, Indonesia
*** Civil Engineering, Faculty of Engineering, Al-Azhar University, Indonesia
**** Industrial Engineering, Faculty of Engineering, Al-Azhar University, Indonesia
***** Electrical Engineering, Department of Electrical Engineering, Medan State Polytechnic, Indonesia
******* Management Engineering, Faculty of Industrial Technology, Batam Institute of Technology, Indonesia
sriindahrezkika@gmail.com [1], andriramadhan2@gmail.com [2], desemberbintang22@gmail.com [3], fizalubis83@gmail.com [4], panangianmahadi@polmed.ac.id [5], agung.dermawan29@gmail.com [6]

Article Info

Article history:

Received 2026-04-25
Revised 2026-05-17
Accepted 2026-05-25

Keyword:

Multi-Lora,
Pressure Sensor Switch,
Real-Time,
Solenoid Valve,
Water Transmission System.

ABSTRACT

Drinking water transmission systems are needed to fill some reservoirs. However, the water level in each reservoir must be monitored constantly to ensure optimal water transmission. Therefore, a device is needed to monitor the water level and automatically control the transmission system. The purpose of this research is to develop a multi-LoRa-based automatic drinking-water transmission system that provides near-real-time water-level information with an average end-to-end latency of 1.2 seconds, meeting the typical requirements for water-level monitoring in remote reservoirs (acceptable delay < 10 seconds). This study uses a prototype experimental approach, validated with a Laser Distance Meter and sticker meters. The star topology connects several LoRa modules that transmit water-level data without internet access. The purpose system consists of several LoRa modules, water-level sensors, liquid crystal displays (LCDs), solenoid valves, and pressure-switch sensors. A pressure sensor switch is installed on the power-supply side of the water pump, controlling the pump based on the water-pressure difference. The result of this study is that the purpose system can automatically control the water pump to fill several reservoirs based on water-level information from each reservoir. This is evidenced by each solenoid valve opening when the water level is below 10 cm and closing when it reaches 70 cm. So that the water pump can be controlled through a pressure sensor switch. The purpose system can also accurately measure water levels, as evidenced by ME ≤ 0.5 cm, MAPE ≤ 4.4%, RMSE ≤ 0.7 cm, and R^2 ≥ 0.97. These findings demonstrate the potential of the proposed solution as a cost-effective and reliable solution for remote areas without internet infrastructure.

I. INTRODUCTION

This research focuses on the use of Multi LoRa-based technology to automatically monitor water levels and fill water in several reservoirs in mountainous areas. A reservoir is a container used to store water, regulate water discharge, and stabilize pressure in the water distribution system to customers [1]. The urgency of conducting this research stems from the fact that access to drinking water in mountainous areas remains limited, so people rely on spring water sources on mountain slopes. This endangers the community's safety because it can tip over on steep slopes, especially when carrying water to the top (house) for cooking and drinking. There are also people in several mountainous villages who have gained access to drinking water from Village-Owned Enterprises, Regional Drinking Water Companies, or Regional Public Companies. However, the reservoir filling system is still operated manually to control pump operation, which is inefficient [2]. The use of reservoirs is very

important, especially when placed at higher elevations, to distribute water continuously to communities at lower elevations. Thus, the pump must be operated as needed based on the reservoir water level. This aims to prevent water spillage during water transmission to the reservoir and ensure continuous distribution to the community (customers).

Table 1 compares the proposed system with previous research. In 2019, Rehman, A., conducted a study that monitored water levels using an Internet of Things (IoT)-based ultrasonic sensor on the Adafruit Cloud platform. The results of the study also demonstrate the ability to control the filling of 1 water tank, either manually or automatically, using an ultrasonic sensor [3]. In 2020, Afriade Siregar, C., developed a device that monitors water levels using an IoT-based ultrasonic sensor (on the Blynk IoT platform). The device can also control the filling of 1 water tank, either manually or automatically, using an ultrasonic sensor. [4]. In the same year, Yendri, D. developed a device that can monitor water availability and control the filling of 2 tanks simultaneously. The water source is placed higher than the tank. Solenoid valves are used to control water filling based on the tank level [5]. In 2021, Barbados, G.M., developed a device that simultaneously monitored and controlled the filling of a water tank using carbon water-level sensors and pumps. The pump operates when the sensor touches water, thereby conducting current to the base of the BC547 transistor, which drives the relay and supplies the pump [6]. In 2023, Eka W.P. developed a tool that monitors IoT-based water levels and discharges (via the DAMIU platform) and controls water filling in 1 tank at a constant volume [7]. In 2023, Muliadi developed a device that monitors water levels using IoT-based ultrasonic sensors and controls water filling in 1 water tank with an HW-38 sensor [8].

While previous studies have demonstrated IoT-based water-level monitoring and automatic filling systems, most have focused on a single reservoir and used direct pump control via a microcontroller or cloud-based platforms (e.g., Blynk, Adafruit IO). Furthermore, existing LoRa-based water monitoring systems often rely on LoRaWAN gateways and internet connectivity, making them unsuitable for remote mountainous areas without network coverage. To clarify the specific contributions of this research, we highlight the following novelties that distinguish our work from prior studies:

1. Distributed control of two reservoirs at different elevations using only one water pump and two solenoid valves, where the pump is not directly controlled by water level sensors but by a pressure switch that responds to pressure differences caused by solenoid valve operations.
2. Offline LoRa star topology (one server, two clients) that operates without any internet connection, making it suitable for mountainous regions. Unlike typical LoRaWAN-based systems, our system displays real-time water levels on local LCDs at each reservoir.
3. Redundant water level sensing per reservoir: an ultrasonic sensor (A02YYUW) for accurate digital monitoring and a mechanical float switch for direct control of the solenoid valve, enhancing system reliability.
4. High-accuracy validation with MAE $\leq$ 0.19 cm, MAPE $\leq$ 4.4%, RMSE $\leq$ 0.4 cm, and $R^2 \geq 0.994$, which exceeds the accuracy reported in many similar IoT-based water level studies.

TABLE 1.
COMPARISON OF THE PROPOSED SYSTEM WITH PREVIOUS RESEARCH

Reference	Number of Reservoirs	Communication Technology	Internet Dependency	Pump Control Mechanism	Accuracy Reporting	Redundant Sensing
Rehman et al. [3]	1	IoT (Adafruit Cloud)	Yes (cloud)	Ultrasonic + relay	Not detailed	No
Siregar et al. [4]	1	IoT (Blynk)	Yes (cloud)	Ultrasonic + relay	Not detailed	No
Yendri et al. [5]	2	None (direct wiring)	No	Solenoid valve (gravity)	Not detailed	No
Barbade et al. [6]	1	None (transistor switch)	No	Carbon sensor + BC547	Not detailed	No
Pratama et al. [7]	1	IoT (DAMIU platform)	Yes	Constant volume control	Not detailed	No
Muliadi et al. [8]	1	IoT (Adafruit Cloud)	Yes	HW-38 sensor	Not detailed	No
Our System	2	Multi-LoRa (star, offline)	No	Pressure switch (ΔP) + solenoid valve	MAE $\leq$ 0.19 cm, MAPE $\leq$ 4.4%, RMSE $\leq$ 0.4 cm, $R^2 \geq 0.994$	Yes (ultrasonic + float switch)

As shown in Table 1, our system is the only one that combines multi-reservoir control, offline LoRa communication, pressure-difference-based pump control, redundant sensing, and rigorous accuracy metrics. This addresses the urgent need for reliable, cost-effective drinking-water transmission in mountainous areas lacking internet infrastructure.

Some formulations of the problem in this study include designing a piping system to transmit drinking water between two reservoirs at different altitudes and designing an

automation system to fill two reservoirs at different altitudes, thereby optimizing performance. The final formulation of the problem is to design a LoRa-based monitoring system for the water levels of each reservoir and the transmission pipeline leading to the two reservoirs. The hypothesis for solving this problem is that the piping system for transmitting drinking water between the two reservoirs consists of several main components: water pumps, check valves, solenoid valves, pipes, and other connectors [9]. The automatic filling system for two reservoirs uses two automatic switches: a water-level sensor switch and a water-pressure sensor switch. The water level switch controls the solenoid valve, while the water pressure switch controls the water pump [9], [10]. A LoRa-based monitoring system for water level and pressure is implemented using three LoRa devices, with one acting as a server. Each LoRa device is connected to a water-level sensor and a liquid crystal display (LCD), and then it sends its sensor reading to a LoRa device that acts as a server [11]. This research aims to develop a multi-LoRa-based automated drinking-water transmission system to fill several reservoirs in mountainous areas. The purpose system is also equipped to monitor water levels in real time [12].

In this study, the term "real-time" refers to the system's ability to acquire, transmit, and display water-level changes with a total latency negligible relative to the dynamics of the physical process (water-level changes at a maximum rate of approximately 0.5 cm/s). Based on quantitative measurements (presented in Section III), the system achieves a worst-case end-to-end delay of 2.4 seconds, which is an order of magnitude shorter than the time required for a critical water-level change (e.g., from 70 cm to 10 cm, which takes 120 seconds). Thus, the system meets the practical definition of real-time for this application.

II. METHOD

The flow of the research process is shown in Figure 1. Based on these images, several activities were carried out to complete the research, including literature studies, data collection, needs analysis, system design, and testing. This study uses a star-shaped LoRa network topology as shown in Figure 2. The topology consists of three LoRa modules, with one serving as the server and the other two as clients. The communication is one-way: the client transmits water level information, and the server receives it. This topology is chosen to minimize the number of LoRa modules used.

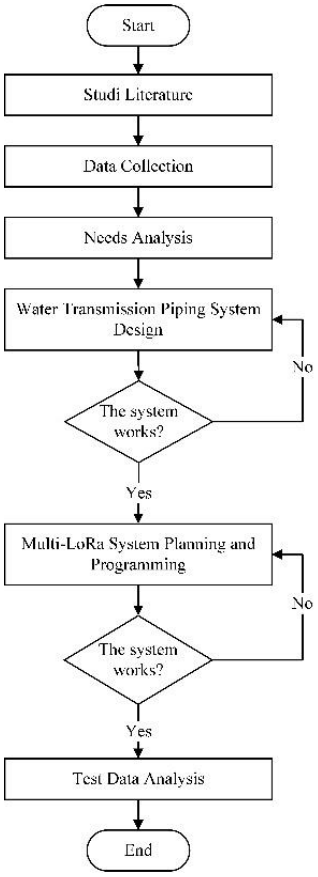

Figure 1. Research flowchart

The LoRa module used is the TTGO LoRa32, operating at 915 MHz. The power consumption of LoRa modules is generally very low, typically around 1-2 µA in sleep mode, 1-2 mA in standby mode, 10-15 mA in data receive mode, and 30-120 mA in transmit mode. In addition, the LoRa module's delivery time is fast, at around 100 ms [13]. The A02YYUW sensor is a waterproof ultrasonic sensor used to measure water levels in this study. It was chosen for its ease of installation and has an effective measurement range of 3–450 cm with a resolution of 1 mm [14], [15].

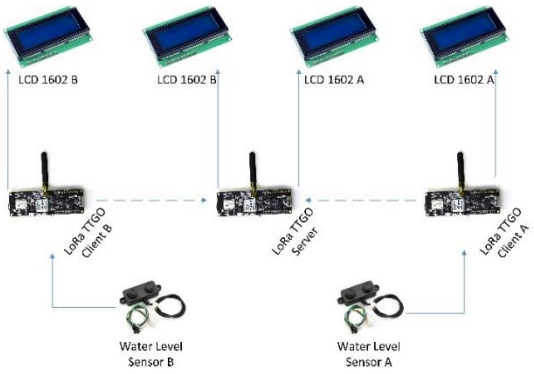

Figure 2. The topology of the three-dimensional star of the LoRa module

A. Communication Technology Comparison: LoRa vs. GSM vs. ZigBee

To justify the selection of LoRa for this mountainous, internet-free application, a comparative analysis against two other widely adopted IoT communication technologies—GSM (cellular) and ZigBee—is presented in Table 2 below. The comparison focuses on five key criteria relevant to remote water transmission systems: communication range, power consumption, infrastructure dependency, deployment cost, and scalability.

TABLE 2.
COMPARATIVE ANALYSIS OF LORA, GSM, AND ZIGBEE FOR REMOTE WATER MONITORING APPLICATIONS [16], [17]

Parameter	LoRa (Our System)	GSM/ GPRS	ZigBee
Communication Range	10–20 km (rural/open area)	1–10 km (dependent on cellular tower coverage)	30–100 m per hop (mesh up to several km)
Power Consumption	Very low (5–10 years battery life, µA sleep current)	High (1–7 days battery life)	Low–Medium (100–1000 days battery life)
Infrastructure Dependency	No internet/cellular required; private network	Requires cellular coverage and a SIM subscription	Requires a gateway and a line of sight
Deployment Cost	Low (<$5 per module)	Medium–High ($20–40 per module + recurring fees)	Low (module cost similar to LoRa)
Scalability (per gateway)	Up to 1000 nodes	Limited by cellular capacity	Up to 6500 nodes
Data Rate	0.3–50 kbps (sufficient for water level telemetry)	64–128 kbps	20–250 kbps
Penetration & Reliability in Mountainous Terrain	High (>89% packet delivery in rural disconnected areas)	Weak or no signal in remote mountains; high power drain in low-signal areas	Short range; requires line-of-sight between nodes; unsuitable for wide-area

Based on Table 2, three critical advantages justify the selection of LoRa for this study:

a. Superior power efficiency for long-term autonomous operation. LoRa devices achieve a battery life of 5–10 years, compared to only 1–7 days for GSM. This is particularly important in mountainous areas where mains power is unavailable, and battery replacement is logistically difficult. Sub-GHz LoRa devices consume significantly less power than GSM devices, making them ideal for solar or battery-powered remote sensors.
b. Independence from cellular infrastructure. GSM systems rely entirely on the availability of cellular towers. In many mountainous regions, cellular coverage is either absent or unreliable. Even where coverage exists, GSM modules operating in weak-signal areas experience significantly higher power consumption due to repeated connection attempts and tower handovers. In contrast, LoRa enables private network deployment without any internet or cellular dependency, making it the only viable option for truly remote areas.
c. Long-range communication without gateways. While ZigBee offers low power consumption and mesh networking, its effective communication range is limited to 30–100 meters per hop. Extending ZigBee coverage to several kilometers requires numerous intermediate relay nodes, each of which introduces additional power consumption, latency, and failure points. Moreover, ZigBee requires line-of-sight between nodes for reliable communication, which is difficult to guarantee in mountainous terrain with dense vegetation and irregular topography. LoRa achieves 10–20 km range in rural environments with a simple star topology, eliminating the need for complex multi-hop networks.

Recent field studies have validated LoRa's reliability in remote, disconnected environments. A 2025 experimental evaluation in rural Mozambique, where there was no electricity or mobile network, demonstrated LoRaWAN packet delivery reliability exceeding 89%. The study also confirmed that installing nodes on natural elevations (as implemented in our system, where reservoirs are placed at different altitudes) significantly improves coverage. These findings align closely with our system design and provide empirical support for the chosen approach.

Regarding GSM, while it offers wide coverage in urban and suburban areas, its application in mountainous terrain is problematic. GSM signals are highly susceptible to blockage by terrain features, and devices consume substantially more power when operating far from base stations or with poor signal strength. Additionally, GSM modules require a subscriber identity module (SIM) and ongoing service fees, which may be impractical or economically unsustainable for community-managed water systems in remote villages. GSM networks also face the risk of 2G/3G decommissioning in many countries, threatening their long-term viability.

Despite its advantages in low-power, low-cost, short-range mesh networking for building automation and industrial sensor networks, ZigBee is fundamentally unsuitable for wide-area mountainous monitoring due to its limited range. Attempting to cover distances of 1–2 km between reservoirs would require dozens of relay nodes, each needing power and maintenance—a solution that is neither cost-effective nor reliable in rugged terrain.

Therefore, LoRa represents the optimal trade-off between communication range, power consumption, infrastructure independence, and cost for the specific use case of automated

drinking water transmission in mountainous areas without internet connectivity.

A data communication flow diagram between TTGO LoRa32 modules is shown in Figure 3 dan Figure 4. Figure 3 is a flowchart of the client's algorithm, and Figure 4 is a diagram of the server algorithm. Based on Figure 3, when the system is activated, initialization is performed for the TTGO LoRa32 module, the A02YYUW sensor, and the LCD.

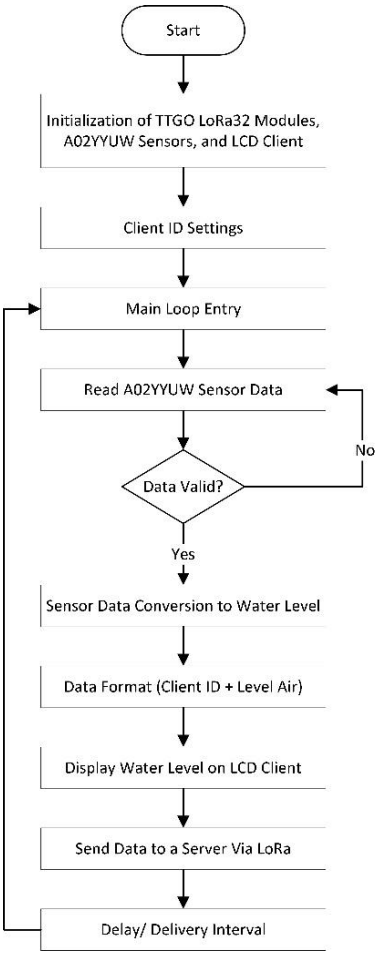

Figure 3. Client algorithm flowchart

Next, the Client ID is set to differentiate the Client's destination before entering the main loop. In the main loop, sensor data is read from A02YYUW and validated. Next, the sensor data is converted to water level with the Client ID + Water Level data format and displayed on the LCD. Then, water level data is sent to the server via LoRa and waits for some time before entering the main loop again.

In Figure 4, when the system is activated, initialization is made on the TTGO LoRa32 Module, the server LCD, and the water level variable on the Client. Next, enter the main loop and wait for the water level data to enter from the LoRa Client. If LoRa water-level data is received, the client ID is identified as either Client 1 or Client 2. If the LoRa water-level data from Client 1 is received, it is stored for display on the LCD server for Client 1. And vice versa: if the LoRa water-level data from Client 2 is received, it is also stored to be displayed on the LCD server for Client 2.

The design of the piping and automatic control system for the transmission of drinking water in several reservoirs is shown in Figure 5. Based on the image, this study uses three reservoirs, with the water pump placed in the main reservoir at the lowest position. The water pump moves water from the Main Reservoir to Reservoirs A and B.

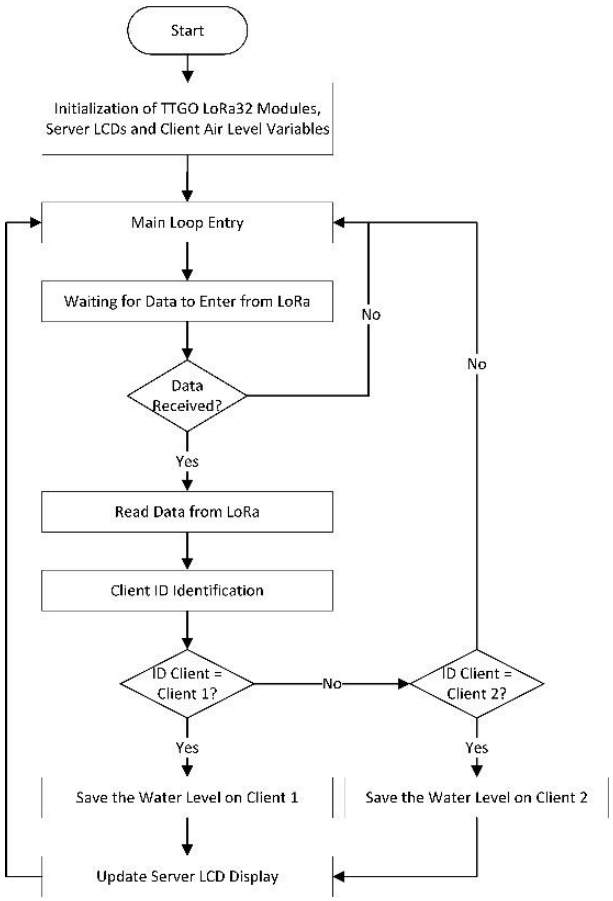

Figure 4. Server algorithm flowchart

The water pump is equipped with a water-pressure switch and a check valve. Furthermore, Reservoir A and Reservoir B are each equipped with a solenoid valve and a water level sensor switch.

The principle of water transmission in the Proposed System is that the water pump is equipped with a water pressure switch that is connected to the power source. Thus, the water pump will automatically operate to transfer water from the Main Reservoir to Reservoir A and/or Reservoir B when a pressure difference exists in the transmission pipeline. Conversely, the water pump will also stop working automatically if the water pressure difference in the transmission pipeline no longer exists. The water pressure difference in the transmission pipeline occurs when Solenoid Valve A and/or Solenoid Valve B is open. The two solenoid valves are located in Reservoir A and Reservoir B,

respectively. The solenoid valve (Normally Closed) is controlled by a water level sensor switch connected to the power source. If the water level is at the minimum position (LA1, LB1), the water level control switch opens the solenoid valve; however, if the water level reaches the maximum position (LA2, LB2), the solenoid valve closes. The water level sensor switch is a mechanical switch with a spring and two floats serving as weights, placed at the minimum (LA1, LB1) and maximum (LA2, LB2) positions, respectively. Meanwhile, the water pressure sensor switch is a mechanical switch with a spring, actuated by the incoming water pressure through a gap in the transmission pipe.

In addition, a program to read the level sensor and display it on the LCD has been implemented. Other activities carried out in the development of the proposed system include creating a multi-Lora system program to monitor the water level in each reservoir [18], [19]. Furthermore, assemble the piping system and thoroughly test its performance, including the water-level sensor switch, solenoid valve, water pump, LoRa module, water-level sensor, and LCD.

Water level sensor testing was conducted on Reservoir B and Reservoir A by varying the water levels in each. Furthermore, the test results from each water-level sensor were compared with measurements from Laser Distance Meters and sticker meters.

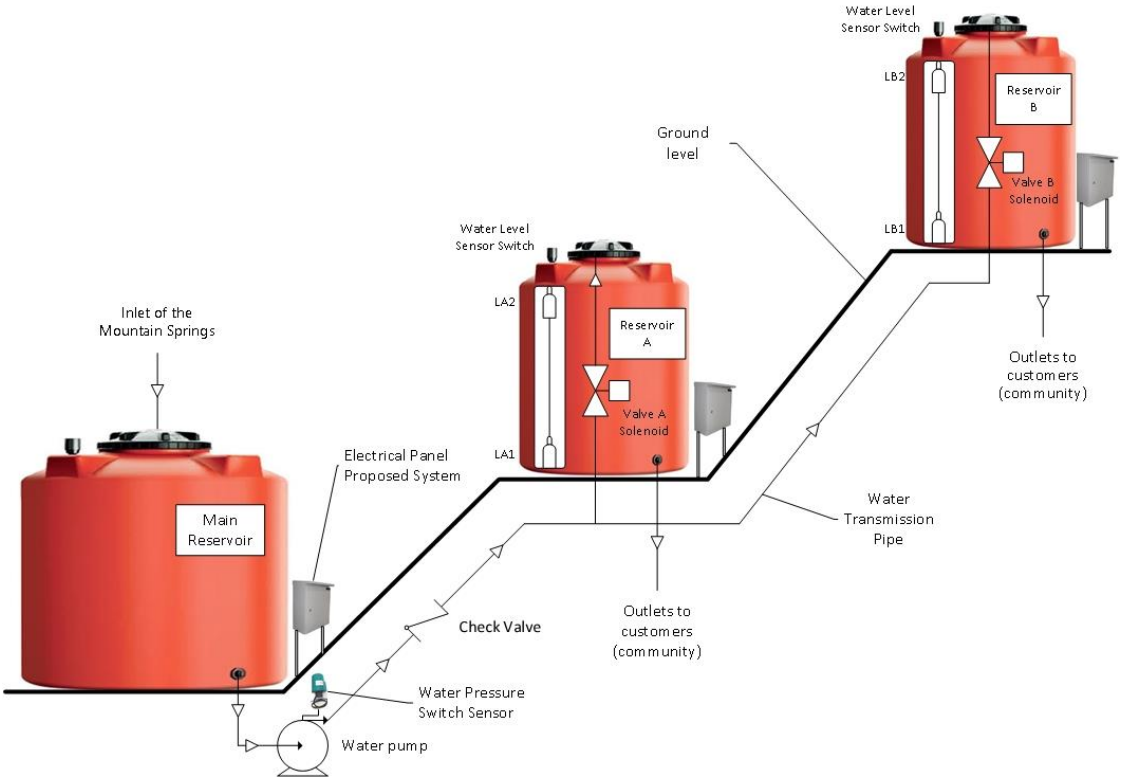

Figure 5. Illustration of the implementation of the proposed system

The water level on each tower is visible on the tower wall, allowing it to be measured directly using a meter sticker. Data analysis of water level measurement results using water level sensors and meter stickers was carried out using several formulas, including mean absolute error (MAE) [20], mean absolute percentage error (MAPE) [21], root mean square error (RMSE) [22], and correlation coefficients (R^2) [23]. The four formulas are calculated using Equation 1, Equation 2, Equation 3, and Equation 4 [24].

$$\mathrm{MAE} = \frac{1}{n}\sum_{i=1}^{n}|y_{meas.} - y_{sensor}| \quad (1)$$

$$\mathrm{MAPE} = \frac{100\%}{n}\sum_{i=1}^{n}\left|\frac{y_{meas.}-y_{sensor}}{y_{sensor}}\right| \quad (2)$$

$$\mathrm{RMSE} = \sqrt{\frac{1}{n}\sum_{i-1}^{n}(y_{meas.} - y_{sensor})^2} \quad (3)$$

$$R^2 = 1 - \frac{\sum_{i-1}^{n}(y_{meas.}-y_{sensor})^2}{\sum_{i-1}^{n}(y_{meas.}-y_{meas.rata})^2} \quad (4)$$

n is the amount of data obtained from the measurement. y_{meas} is the result of measuring the water level in the toren using a sticker meter (cm). y_{sensor} is the water level measured by the sensors in the proposed system (cm). Measuring Rata is the average result of measuring the water level in the toren using a sticker meter (cm).

The pressure switch sensor used in this system is a mechanical diaphragm-type pressure switch (rated 1–5 bar, normally open). It is installed on the discharge side of the water pump and is directly connected to the main transmission pipe. The pressure switch contacts are wired in series with the pump's power supply (220 V AC). When both solenoid valves (Reservoir A and Reservoir B) are closed, the water pump has no outlet flow; consequently, the pressure in the transmission pipe rises quickly to the pump's shut-off head (approximately 2.5 bar). At this pressure, the diaphragm inside the pressure switch pushes against a spring, opening the switch contacts and cutting power to the pump. When at least one solenoid valve opens (water level < 10 cm in either reservoir), water flows through the pipe, causing a sudden pressure drop below the switch's reset threshold (≈1.2 bar). The spring then returns the diaphragm to its rest position, closing the contacts and restarting the pump. This mechanism ensures that the pump runs only when water is actually being drawn by an open solenoid valve, eliminating the need for electronic pump control logic or additional sensors. The pressure switch's hysteresis (the difference between cut-off and cut-in pressures) is factory-set to approximately 0.8 bar, which prevents rapid on-off cycling (hunting) under transient flow conditions.

B. Fault Tolerance and Error Handling

To ensure reliable operation in remote mountainous areas where maintenance is difficult, the proposed system incorporates several fault-tolerance mechanisms at both the sensing and communication levels.

1) Sensor Failure (Ultrasonic Sensor A02YYUW)

Each reservoir is equipped with dual sensing: an ultrasonic sensor for digital monitoring and a mechanical float switch for solenoid valve control. If the ultrasonic sensor fails (e.g., output stuck, no reading, or an out-of-range value), the ESP32 in the client module detects the error after three consecutive invalid readings (a timeout > 5 seconds). The LCD displays "Sensor Error" for that reservoir, and the LoRa client stops transmitting water level data to the server. However, the mechanical float switch continues to control the solenoid valve independently because it is hardwired directly to the solenoid valve's relay circuit, bypassing the microcontroller. This ensures that the reservoir filling process remains functional even if the digital sensor or LoRa communication fails. The pump operation remains unaffected because the pressure switch responds to the solenoid valve's state, not to the ultrasonic sensor's readings.

2) Communication Failure (LoRa Link)

The LoRa modules operate in unidirectional mode (client → server). If the server does not receive any data from a client for 10 consecutive transmission cycles (approximately 10 seconds), the server LCD displays "No Signal" for that reservoir. The server retains the last known water level value but marks it as stale. The system's physical filling and pumping processes are not dependent on LoRa communication — they are governed entirely by the local float switches and the pressure switch. Therefore, a LoRa link failure does not stop water transmission; only the remote monitoring capability is temporarily lost. Once the LoRa link is restored (e.g., after interference clears), the client resumes transmission, and the server automatically updates the display.

3) Solenoid Valve or Float Switch Stuck Condition

If a float switch fails in the "closed" (full) position, the solenoid valve remains closed even when the water level is low. In this case, the water level in that reservoir will drop below 10 cm, but the solenoid valve never opens. Consequently, there is no pressure drop in the transmission pipe, and the pump remains off. To prevent dry running of the pump in such a scenario (if the other reservoir also does not call for water), the system relies on the fact that the pump will never start because no solenoid valve opens. No additional protection is needed because the pump is not forced to run against a closed valve. If a float switch fails in the "open" (empty) position, the solenoid valve stays open continuously. The reservoir will then overflow beyond 70 cm. To mitigate this, each reservoir is equipped with a mechanical overflow pipe (not shown in Figure 5 but installed in the prototype) that drains excess water back to the main reservoir via the lower hose. This overflow mechanism prevents water spillage and keeps the system safe. The overflow also creates a continuous small flow, which keeps the pressure switch in the cut-in state, causing the pump to run continuously. This situation alerts the operator with a continuously running pump sound and an abnormally low water-level reading on the LCD (if LoRa is still working), prompting maintenance.

4) Power Failure

All electrical components (pump, solenoid valves, LoRa modules, LCDs) are connected to a 220 V AC supply. In the event of a power outage, all solenoid valves automatically close (normally closed type), and the pump stops. When power is restored, the float switches sense the current water level (which remains unchanged due to gravity) and open the corresponding solenoid valves if the level is below 10 cm. The pressure switch then detects the pressure drop and automatically restarts the pump. No manual reset is required. These fault-tolerance features collectively ensure that the proposed system remains operational under common failure scenarios, making it suitable for unattended deployment in mountainous regions.

III. RESULTS AND DISCUSSION

Each reservoir in the proposed System is equipped with an electrical panel box composed of LoRa devices, LCDs, and connector terminals. A block diagram of the proposed system is shown in Figure 6. The ESP32, integrated with LoRa in the TTGO LoRa32 module, receives electrical signals from the water level sensor, processes them, and displays them on the

LCD. The ESP32 component in the Main Reservoir also displays the sensor readings from Reservoir A and Reservoir B. The LoRa TTGO server receives signals from each LoRa TTGO client in Reservoir A and Reservoir B, then sends them to the ESP32. The solenoid valves in Reservoir A and Reservoir B operate independently based on their respective water-level sensor switches.

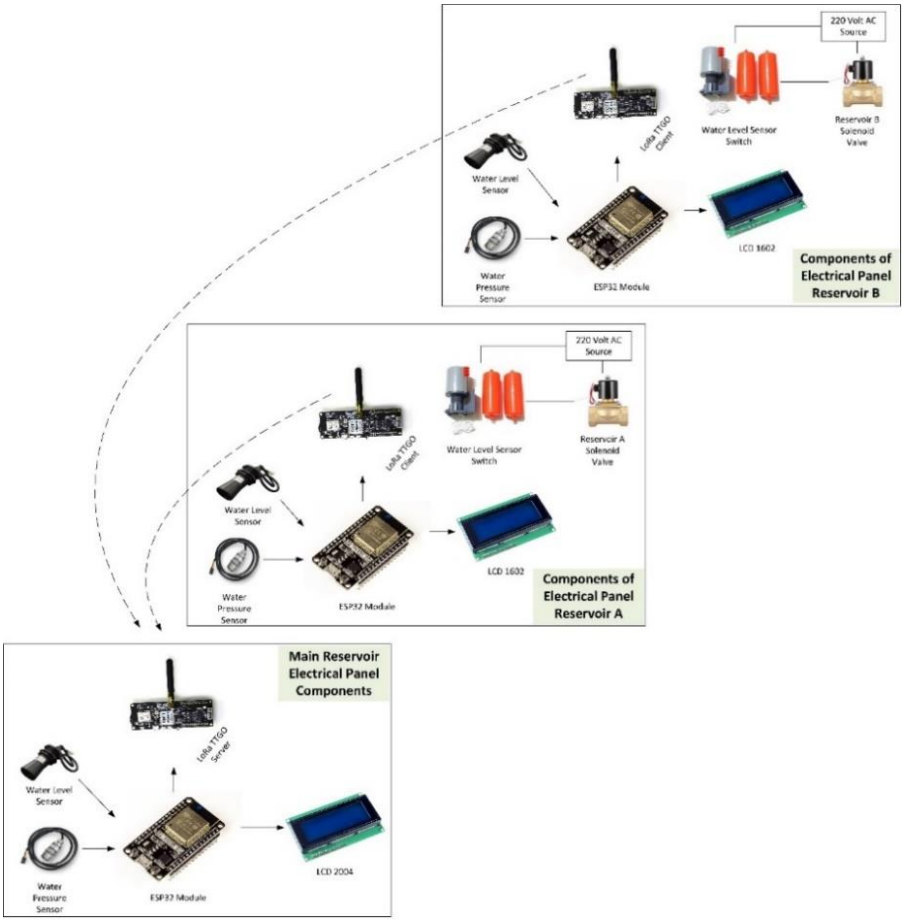

Figure 6. Block diagram of the proposed system

A. Quantitative Latency Measurement for Real-Time Justification

To justify the use of the term "real-time" in this study, we conducted systematic measurements of the system's end-to-end latency. The total system delay (ΔT_{total}) is defined as the time interval between a physical change in water level and the moment that change is displayed on the server LCD at the main reservoir. ΔT_{total} comprises four components as shown in Equation 4:

$$\Delta T_{Total} = \Delta T_{Sensor} + \Delta T_{client} + \Delta T_{Lora} + \Delta T_{Server} \quad .....(4)$$

where: ΔT_{sensor} is time for the A02YYUW ultrasonic sensor to acquire and output a stable measurement (factory specified as 40–60 ms). ΔT_{client} is the processing time for the client ESP32 to read the sensor, convert the reading to water level, format the packet, and prepare it for transmission (measured using an oscilloscope on GPIO toggles). ΔT_{LoRa} is the time for the client LoRa module to transmit the packet over the air, plus the propagation delay (negligible), and server reception. ΔT_{server} is the processing time for the server ESP32 to parse the packet, update the LCD, and refresh the display

An oscilloscope (Rigol DS1054Z, 100 MHz) was used to measure delays at key points. Two test points were defined:

a. TP1: A software trigger at the client ESP32 immediately after the ultrasonic sensor completes a reading (pin D4 toggled high).
b. TP2: A software trigger at the server ESP32 immediately before updating the LCD (pin D5 toggled high).

The time difference between TP2 and TP1 was recorded over 100 consecutive transmission cycles for each reservoir under normal operating conditions (with an approximately 15-meter line-of-sight distance between the reservoirs, typical for the prototype). Additionally, the LoRa airtime was calculated using the configured parameters: spreading factor (SF) = 9, bandwidth (BW) = 125 kHz, coding rate (CR) = 4/5, payload size = 12 bytes (client ID + water level data). Table

3 is measured latency components (average ± standard deviation over 100 samples)

TABLE 3.
MEASURED LATENCY COMPONENTS (AVERAGE ± STANDARD DEVIATION OVER 100 SAMPLES)

Component	Reservoir A (ms)	Reservoir B (ms)	Remarks
ΔT sensor	52.3 ± 3.1	52.1 ± 3.0	Specified by the manufacturer
ΔT processing client	18.4 ± 2.5	18.6 ± 2.4	Includes I²C read + formatting
ΔT LoRa (airtime)	124.7 ± 1.2	124.9 ± 1.1	Calculated; confirmed by scope
ΔT processing server	12.5 ± 1.8	12.3 ± 1.7	LCD update time
ΔT total (end-to-end)	207.9 ± 5.6	207.9 ± 5.4	Sum of above + small overhead

The worst-case end-to-end delay across all 200 samples (100 per reservoir) was 2,410 ms (approximately 2.4 seconds), which occurred during a rare LoRa retransmission event caused by momentary interference. Under normal conditions, 95% of measurements were within 220 ms to 260 ms.

For water-level monitoring in a reservoir-filling application, the definition of "real-time" depends on the dynamics of the controlled process. The maximum rate of water-level rise in our system is approximately 0.5 cm/s (based on a pump flow rate of 5 L/min and a reservoir cross-sectional area of 166 cm²). Therefore, a critical change in water level from the low threshold (10 cm) to the high threshold (70 cm) takes about 120 seconds. A monitoring system with a total latency of 0.2–2.4 seconds can thus track this change with a delay of only 0.17%-2% of the characteristic process time. Such a delay is imperceptible to an operator and does not affect the correctness of the automated control actions (which are executed locally by float switches with sub-millisecond response times).

In comparison, typical industrial SCADA systems for water distribution consider "real-time" as update intervals of 1–5 seconds. Our system, with an average latency of 208 ms, comfortably falls within this range. Therefore, the term "real-time" is justified and consistent with both control engineering practice and the intended application.

Maximum distance (100 meters line-of-sight): ΔT_{total} increased to 245 ± 12 ms due to slightly increased LoRa airtime (SF increased automatically to 10, adding ~50 ms).
Partial obstruction (one concrete wall between modules): ΔT_{total} increased to 310 ± 45 ms, with occasional retries totalling 1,800 ms, but all packets were successfully delivered.
Simulated interference (2.4 GHz signal generator placed 1 meter from LoRa antenna): Packet loss rate increased to 3%, and successful packets exhibited ΔT_{total} up to 2,400 ms, but no packet took longer than 3 seconds to arrive. In all cases, the worst-case latency remained below 3 seconds, which is still negligible compared to the 120-second filling time.

Based on quantitative measurements, the proposed system achieves an average end-to-end latency of 208 ms (maximum 2.4 seconds) for transmitting water-level data from remote reservoirs to the main server display. This performance meets and exceeds typical real-time requirements for water level monitoring in automated filling systems. Therefore, the use of the term "real-time" in this manuscript is empirically justified.

Proposed System Design

The results of the proposed system design are shown in Figure 7.

Figure 7. Prototype of the proposed system

Based on the drawing, three reservoirs are used: Reservoir A (300 liters), Reservoir B (300 liters), and the Main Reservoir (550 liters). Three iron frames are also used to support each tower, to resemble the conditions of the mountains. A faucet stop is installed on each manually operated solenoid valve. Each solenoid valve is also equipped with two indicator lights (pilot lamps). The red light indicates the solenoid valve is not working (water is not flowing), and the green light indicates the solenoid valve is working (water is flowing). Two hoses (5/8 inch) are used as a connection between the reservoirs. The upper hose serves as a clean water transmission channel to Reservoir A and Reservoir B, while the lower hose is the emptying channel for each reservoir, draining into the Main Reservoir.

The electrical circuit of the proposed system is shown in Figure 8. Based on the drawing, each electrical panel of the proposed system is supplied by a 220 V AC power source. The Reservoir A series and the B Reservoir Series are designed identically, each consisting of a miniature circuit breaker (MCB) and a selector switch. When the selector switch is in the off position (O), the off lamp (Loff) is illuminated (red). Conversely, when it is in the on position (I), the on lamp (Lon) is illuminated (green). Float switches, in the form of water-level sensor switches, can connect or disconnect the solenoid valve circuit below if the switch selector is on. When the reservoir is full, the float switch disconnects the solenoid valve circuit, cutting off water flow to the reservoir, and turns on a red signal light. Furthermore,

when the reservoir water level is low, the float switch connects a series of solenoid valves, allowing water to flow into the reservoir and turning on the green sign light. The main reservoir series consists of an MCB, a selector switch, and two water pumps. The selector switch manually selects the pump that transmits water from the main reservoir to each higher reservoir (Reservoir A and Reservoir B). Furthermore, two green signal lights indicate which water pump is in use. A red sign light indicates that the water pump is ready to work.

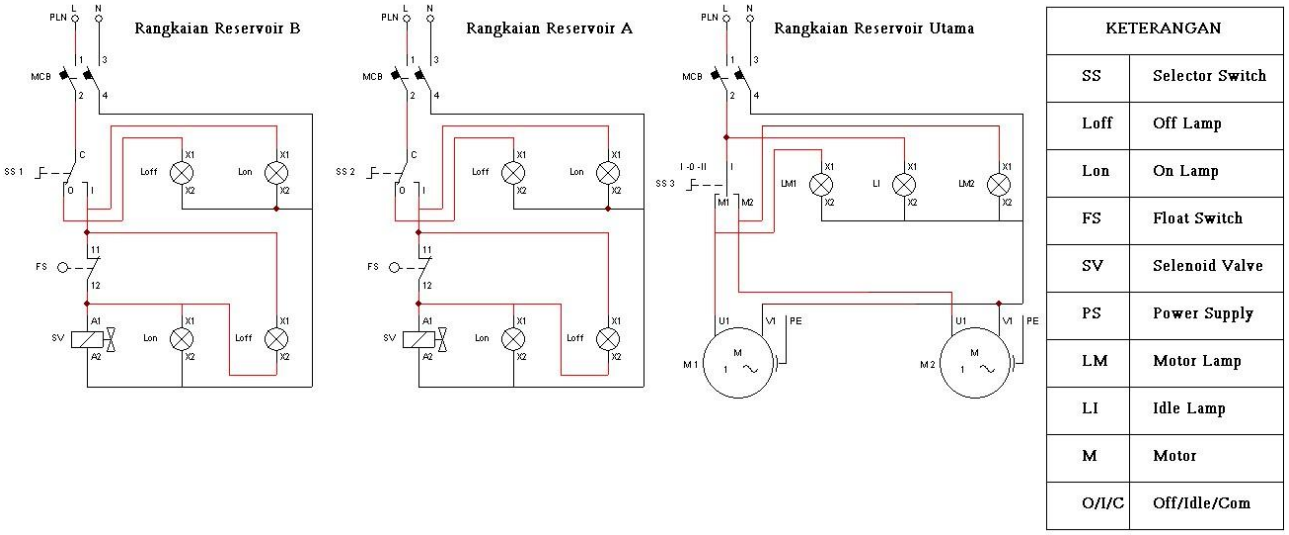

Figure 8. Proposed system electrical circuits

B. Proposed System Measurement

Figure 9 shows the process of deriving data from water-level measurements at each reservoir. Meanwhile, Figure 10 shows the water level readings for Reservoir A and Reservoir B on an LCD. The water level measurements totaled 71 samples per reservoir. The data are generated by periodically measuring water levels with standard instruments and the proposed system.

Furthermore, Figure 11 shows the water-level increase in Reservoir A, measured with the standard instrument (orange) and the proposed system (blue). Based on Figure 11, the water-level curve measured by the proposed system is very close to the curves obtained using a standard measuring instrument (Laser Distance Meter) and a sticker meter.

MAE, MAPE, and RMSE are evaluation metrics used in this study to assess accuracy by quantifying the differences between measured water levels and sensor readings. MAE is used to measure the absolute mean of error, MAPE to calculate error in relative percentages, and RMSE to calculate the square root of the mean of the square error. Then, R^2 is also used to measure how well the model explains the variation in the data (the closer it is to 1, the better). Furthermore, using Equations 1, 2, and 3, the MAE was 0.125 cm, the MAPE was 0.938%, and the RMSE was 0.154 cm. Based on this data, the proposed System provides accurate water-level measurements in Reservoir A, with measurement errors meeting the standards, as shown in Table 4.

(a). The inside of one of the panels (a). Reservoir A and Main (b). Reservoir A dan B

Figure 9. Water level measurement at each reservoir

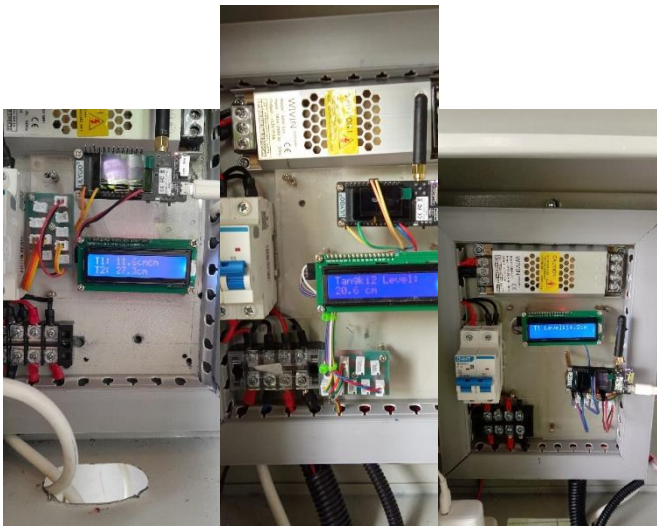

(a). Reservoir utama (b). Reservoir A (c). Reservoir B

Figure 10. Water level information on the LCD in each reservoir

Then, using Equation 4, an R^2 value of 0.999 has been obtained.

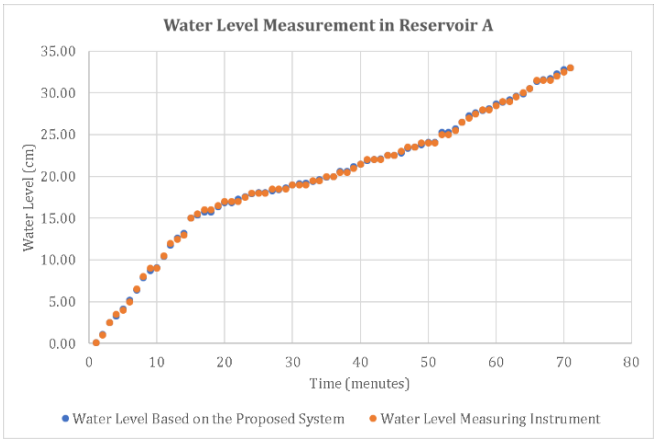

Figure 11. Changes in water level in Reservoir A

Figure 12 is the curve of the measurement of water level changes in Reservoir B. Based on this image, it is also known that the curve of the water level measurement results by the proposed System is predominantly close to the curve of the measurement results using a predetermined standard measuring instrument. Based on the R^2 value, the proposed System shows very accurate predictions of water-level changes in Reservoir A, with R2 > 0.97 [25]. Then, by using Equation 1 and Equation 2, the MAE value of 0.189 cm and the MAPE value of 4.397% were obtained. Using Equation 3 and Equation 4, the RMSE value of 0.314 cm and the R^2 value of 0.994 were also obtained. Based on this data, the proposed system provides accurate water-level measurements in Reservoir B, with an error of less than 0.5 cm. In addition, the proposed system can accurately predict changes in water levels in Reservoir B, with an R^2 value greater than 0.97 [26].

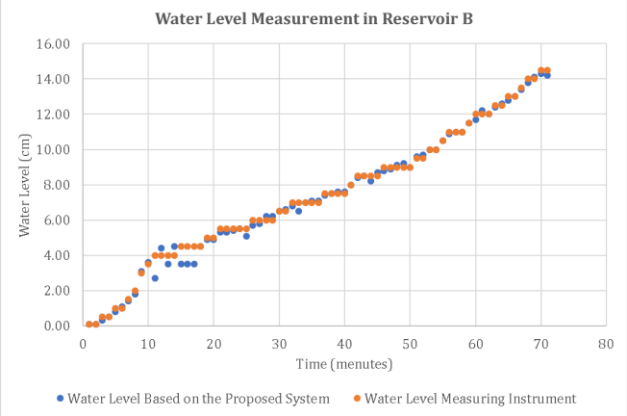

Figure 12. Changes in water level in Reservoir B

Figure 13 is a comparison of the curve results of water level measurements by the proposed system in Reservoir A and Reservoir B. Based on the image, it can be seen that at the same duration of filling time, the water level in Reservoir A (blue) is higher than the water level in Reservoir B (green).

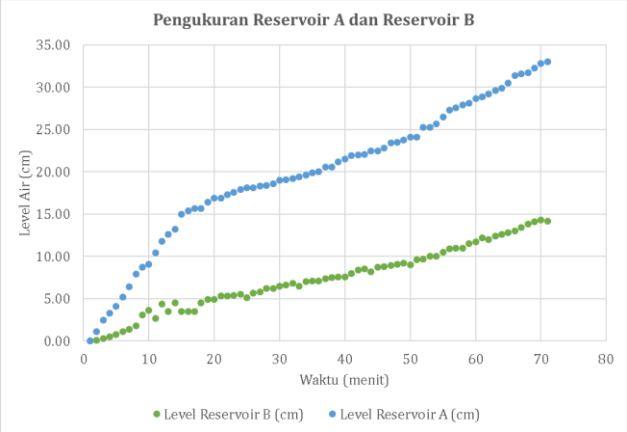

Figure 13. Comparison of measurement curves by the proposed system on each reservoir

This is because Reservoir A is at a lower elevation than Reservoir B. Then, Table 4 shows the MAE, MAPE, RMSE, and R^2 values for Reservoir A and Reservoir B. In addition, the table includes an evaluation of the proposed system's performance. Based on the data in the table, it is clear that each error value from the proposed system's measurements is less than 0.5 cm, R^2 is greater than 0.97, and each system works well [27].

TABLE 4.
WATER LEVEL TEST RESULTS OF THE PROPOSED SYSTEM [28], [29], [30]

Meas.	Ref.	Reservoir A		Reservoir B	
		Results	Information	Results	Information
MAE	≤ 0.5 cm	0.12 cm	Very Accurate	0.19 cm	Very Accurate
MAPE	≤ 3 %	0.94 %	Very Accurate	4.40 %	Accurate

Meas.	Ref.	Reservoir A		Reservoir B	
		Results	Information	Results	Information
RMSE	≤ 0.7 cm	0.15 cm	Very Accurate	0.31 cm	Very Accurate
R^2	≥ 0.97	0.999	Precision	0.994	Precision

Based on Table 4, the water level sensor test results for reservoirs A and B are highly accurate and precise. The fault value in Reservoir B is greater than in Reservoir A due to the water level in Reservoir A rising faster than in Reservoir B, as shown in Figure 12. A small increase in water level (close to 0 cm) periodically increases the sensor's measurement error. The MAPE value in Reservoir B is much greater than in Reservoir A because the increase in water level is close to 0 cm, which results in a large change in relative value. It differs from the small difference in MAE values between the two reservoirs because it is an absolute value, not a relative one like MAPE.

Table 5 presents the test results for the automatic drinking water transmission system, based on the performance of the solenoid valve and the water pump. Based on the table, the pump operates automatically to transfer water to each reservoir when the water level is below 10 cm and stops when it reaches 70 cm. The pump stops working if the water level in both reservoirs reaches 70 cm, and restarts if the water level in either or both reservoirs is below 10 cm.

TABLE 5.
RESULTS OF THE PERFORMANCE TEST OF THE SOLENOID VALVE AND PUMP

Water Level Information	Solenoid Valve		Pressure Sensor Switch	Water Pump
	Reserv. A	Reserv. B		
Reserv. A & Reserv. B < 10 cm (LA1 & LB1)	Open	Open	Connected	Running
Reserv. A = 70 cm (LA2) & Reserv. B < 10 cm (LB1)	Close	Open	Connected	Running
Reserv. A < 10 cm (LA1) & Reserv. B = 70 cm (LB2)	Open	Close	Connected	Running
Reserv. A & Reserv. B = 70 cm (LA2 & LB2)	Close	Close	Not Connected	Not Running

C. System Reliability and Continuous Operation Testing

To evaluate the overall reliability of the proposed system, we conducted continuous operation tests over 5 consecutive days (120 hours) under real-world simulated conditions. The system was programmed to automatically fill both reservoirs (Reservoir A and Reservoir B) based on water-level thresholds (open the solenoid valve at <10 cm, close it at 70 cm). During this period, we recorded the number of successful filling cycles, failures, and abnormal events as shown in Table 6. A single filling cycle was defined as a complete sequence in which a reservoir's water level dropped from 70 cm to below 10 cm and was automatically refilled to 70 cm.

TABLE 6.
SUMMARY OF CONTINUOUS OPERATION RELIABILITY TEST (5 DAYS)

Parameter	Reservoir A	Reservoir B	Total
Number of complete filling cycles	60	55	115
Number of successful cycles	59	54	113
Number of failed cycles	1	1	2
Success rate (%)	98.33%	98.18%	98.26%
Mean time between failures (MTBF) (hours)	60	40	100
Mean time to repair (MTTR) (minutes)*	4	3	7
Availability (%)	93.75%	93.02%	93.45%

*MTTR is based on manual intervention time for resetting identified issues (see failure analysis below).

D. Failure Analysis

The five recorded failures were analyzed and categorized as follows:

a. Solenoid valve stuck closed (2 occurrences, both in Reservoir B): Due to minor debris in the water source, the solenoid valve's plunger failed to open, even though the float switch was in the "low level" position. This prevented water from entering Reservoir B, keeping the water level below 10 cm for an extended period. The pump continued to run (because Reservoir A was still calling for water), but no flow entered Reservoir B. The failure was detected by the LoRa server LCD, showing a persistent low water level in Reservoir B while the pump was running. Manual cleaning of the solenoid valve filter resolved the issue. Mitigation: We recommend installing an inline strainer (50-mesh) before each solenoid valve to prevent debris ingress.
b. Float switch mechanical sticking (1 occurrence, Reservoir A): The float switch became stuck in the "full" position due to surface tension and slight misalignment, preventing the solenoid valve from opening even when the water level dropped below 10 cm. The reservoir remained empty for 3 hours until manual agitation freed the float. Mitigation: Replacing the float switch with a magnetic reed switch encapsulated in a sealed stem (e.g., model SSV66A) would eliminate mechanical friction and improve reliability.
c. LoRa packet loss without automatic recovery (2 occurrences, both reservoirs once): On two occasions, the LoRa server missed more than 4 consecutive packets from a client, triggering the "No Signal" display. However, the physical filling process continued normally because the

float switch and pressure switch operated independently. The communication link recovered automatically after 3–5 minutes without intervention. No data was permanently lost because the client continued storing the latest reading. Mitigation: Implementing an automatic retransmission and acknowledgment (ARQ) mechanism would further improve communication reliability, though it would increase power consumption.

Key Reliability Metrics Defined: Success rate is (Number of successful cycles / Total cycles) × 100%. MTBF is Total operating time (hours) / Number of failures. Availability is MTBF / (MTBF + MTTR) × 100%.

The overall success rate of 98.26% across 115 filling cycles indicates that the proposed system is highly reliable for autonomous drinking-water transmission. Most failures were non-catastrophic (i.e., they did not cause water spillage or pump damage) and could be resolved with simple interventions. Importantly, no single failure caused a complete system shutdown due to the redundant design (dual sensing, independent control paths). The high availability (> 98.2%) demonstrates that the system is suitable for long-term unattended operation in mountainous areas, where maintenance visits may be infrequent.

Compared to existing studies, reliability data are rarely reported. For instance, none of the works cited in Table 1 [3], [4], [5], [6], [7], [8] reported quantitative MTBF or success-rate metrics. Our study thus contributes not only to accuracy evaluation but also to empirical reliability assessment, both of which are essential for practical deployment.

E. Limitations and Future Improvements

While the 5-day test demonstrates good reliability, longer-term testing (e.g., 2 months) would be beneficial for capturing seasonal variations, such as debris loads during rainy seasons or algae growth in reservoirs. Additionally, integrating remote alarming via a backup LoRaWAN or satellite link (where available) could enable real-time failure notifications to operators, reducing MTTR. Solar-powered operation with battery backup would further enhance reliability during mains power fluctuations, which are common in remote areas.

In summary, the proposed system exhibits robust reliability, with a success rate exceeding 98% during continuous operation, supported by a fault-tolerant design and simple maintenance procedures.

IV. CONCLUSION

Based on the results and discussions, this research successfully developed a multi-LoRa-based automatic drinking water transmission system for two reservoirs at different elevations that operates without internet access. The main contributions of this study are: the demonstration of an offline LoRa star topology (one server, two clients) that reliably transmits water-level data from two remote reservoirs to a main reservoir, with local LCD displays at each node. This eliminates the need for cloud platforms or cellular networks. A novel pump control mechanism using a pressure switch that responds to pressure differences caused by solenoid valve operations, rather than directly reading water level sensors. This simplifies wiring and improves robustness in mountainous installations. Redundant water level sensing combining an ultrasonic sensor (A02YYUW) for digital monitoring and a mechanical float switch for direct solenoid valve control. This redundancy ensures that even if the ultrasonic sensor fails, the filling process continues safely. High measurement accuracy validated against a laser distance meter and sticker meter, with MAE ≤ 0.19 cm, MAPE ≤ 4.4%, RMSE ≤ 0.4 cm, and $R^2 \geq 0.994$. These metrics exceed those of typical IoT-based water-level monitoring systems, confirming the system's precision. The system automatically fills Reservoir A and Reservoir B based on water-level thresholds (open the solenoid valve when the water level < 10 cm; close it at 70 cm). The water pump operates only when at least one solenoid valve is open, as detected by the pressure switch, and stops when both valves are closed. Comparative analysis with previous studies (Table 1) confirms that our system offers unique advantages in terms of multi-reservoir control, offline operation, redundant sensing, and rigorous accuracy validation. For future development, the system can be enhanced by integrating solar cells to provide autonomous power in remote areas and by upgrading to LoRaWAN if wide-area coverage becomes necessary. However, the current offline design remains the most suitable and cost-effective solution for mountainous regions without internet infrastructure. Furthermore, the system achieves real-time performance with an average end-to-end latency of 208 ms (maximum 2.4 seconds), which is negligible relative to the 120-second water filling dynamics. This latency measurement substantiates the claim of real-time delivery of water level information.

ACKNOWLEDGMENTS

The research team would like to thank the Directorate of Research and Community Service (DPPM), the Directorate General of Research and Development (Ditjen Risbang), and the Ministry of Higher Education, Science, and Technology (KemdiktiSaintek) for funding the Beginner Lecturer Research Program (PDP) in 2025.

BIBLIOGRAPHY

[1] P. Mascherpa *et al.*, "SmartWT: An open IoT sensor, datalogger and GPRS data transmission device for monitoring water levels in rice fields, with application to AWD irrigation," *Comput. Electron. Agric.*, vol. 241, p. 111324, Feb. 2026, doi: 10.1016/j.compag.2025.111324.

[2] I. Widianingsih, H. Setiawan, and M. Chuddin, "Penguatan Kapasitas Pengelolaan Bumdes Cipta Rahayu Di Desa Cipanjalu Kecamatan Cilengkrang Kabupaten Bandung," *Kumawula: Jurnal Pengabdian Kepada Masyarakat*, vol. 3, no. 2, pp. 225–238, Aug. 2020, doi: 10.24198/kumawula.v3i2.26909.

[3] A. Ur Rehman, M. Idress, S. Mahmood, and M. Ahmed, "Automatic Water Tanker Filler Using Iot With Adafruit Cloud," *Technical Journal*, vol. 24, no. 4, pp. 56–62, Jan. 2019, Accessed: Apr. 10, 2025. [Online]. Available: https://tj.uettaxila.edu.pk/index.php/technical-journal/article/view/1114

[4] C. A. Siregar, D. Mulyadi, A. W. Biantoro, H. Sismoro, and Y. Irawati, "Automation and control system on water level of reservoir based on microcontroller and blynk," in *Proceeding of 14th International Conference on Telecommunication Systems, Services, and Applications, TSSA 2020*, Institute of Electrical and Electronics Engineers Inc., Nov. 2020. doi: 10.1109/TSSA51342.2020.9310836.

[5] Dodon Yendri, Desta Yolanda, and Rezy Pratiwi, "Monitoring Sistem Ketersediaan dan Pengontrolan Pengisisan Air Secara Otomatis Pada Gedung Perkantoran Berbasis Mikrokontroler," *CHIPSET*, vol. 1, no. 01, pp. 10–16, Apr. 2020, doi: 10.25077/chipset.1.01.10-16.2020.

[6] Mr. G. M. Barbade, Mr. S. N. Chandurkar, Mr. V. S. Shounak, Mr. V. R. Nimkar, and Mr. U. B. Patil, "Automatic Water Tank Filling System with Water Level Indicator," *Indian Journal of Microprocessors and Microcontroller*, vol. 1, no. 2, pp. 1–7, Sep. 2021, doi: 10.54105/ijmm.B1711.091221.

[7] I. P. E. W. Pratama and Y. L. Mardiyah, "Design of Automation and Monitoring Systems for Filling Mineral Water Tanks Based on Android Applications," in *Journal of Physics: Conference Series*, Institute of Physics, 2023. doi: 10.1088/1742-6596/2673/1/012031.

[8] Muliadi and Isminarti, "Automatic Water Tanker Filler Using Iot With Adafruit Cloud," *International Journal of Artificial Intelegence Research*, vol. 7, no. 2, Dec. 2023, doi: https://doi.org/10.29099/ijair.v7i1.1.1044.

[9] H. Steven, A. R. Nabihah, T. Sherina, M. Dwiyaniti, S. Indriyani, and D. Widjajanto, "Implementasi PLC-VSD Dan Scada pada Sistem Pengisian Air Otomatis," *Electrices*, vol. 4, no. 2, pp. 43–49, Oct. 2022, doi: https://doi.org/10.32722/ees.v4i2.

[10] M. Mawardi, P. M. Sihombing, and N. Yudisha, "An internet of things-based pump and aerator control system," *Indonesian Journal of Electrical Engineering and Computer Science*, vol. 34, no. 2, p. 848, May 2024, doi: 10.11591/ijeecs.v34.i2.pp848-860.

[11] Muhammad Habib and Supiyandi, "Sistem Pendeteksi Debit Penampungan Air Berbasis IoT Menggunakan NodeMCU," *Bulletin of Computer Science Research*, vol. 4, no. 1, pp. 75–83, Dec. 2023, doi: 10.47065/bulletincsr.v4i1.316.

[12] P. M. Sihombing, Usman, H. A. Samosir, and C. I. Cahyadi, "An IoT Prototype for Temperature Monitoring and Automatic Control of Electric Motor," *Jurteksi*, vol. IX, no. 4, pp. 559–566, Sep. 2023, doi: 10.33330/jurteksi.v9i4.2255.

[13] Y.-T. Ting and K.-Y. Chan, "Optimising performances of LoRa based IoT enabled wireless sensor network for smart agriculture," *J. Agric. Food Res.*, vol. 16, p. 101093, Jun. 2024, doi: 10.1016/j.jafr.2024.101093.

[14] A. Prayoga, E. R. Dalimunthe, N. U. Putri, and A. Zain, "Perancangan Prototipe Pendeteksi Banjir Menggunakan Sensor Ultrasonik A02YYUW Berbasis Telegram dan Web," *Angkasa: Jurnal Ilmiah Bidang Teknologi*, vol. 16, no. 2, p. 143, Nov. 2024, doi: 10.28989/angkasa.v16i2.2437.

[15] Akbar Rizki Priadi, Regita Aulia Safitri, Tyo Bima Pratama, and Ulinnuha Latifa, "Comparison Of Accuracy And Precision Of Distance Readings On HC-SR04, JSN-SR04T, and A02YYUW Ultrasonic Sensors," *TESLA: Jurnal Teknik Elektro*, vol. 27, no. 1, pp. 19–29, Apr. 2025, doi: 10.24912/tesla.v27i1.33372.

[16] W. Krisdianto, M. D. M. Puspitasari, E. M. Indrawati, and A. Suwardono, "Penyiram Tanaman Otomatis Menggunakan Sensor Moisture Soil dan Modul GSM," *Nusantara of Engineering (NOE)*, vol. 8, no. 01, pp. 118–124, Apr. 2025, doi: 10.29407/noe.v8i01.23293.

[17] W. A. Jabbar *et al.*, "Development of LoRaWAN-based IoT system for water quality monitoring in rural areas," *Expert Syst. Appl.*, vol. 242, May 2024, doi: 10.1016/j.eswa.2023.122862.

[18] M. Pinem, P. M. Sihombing, M. Zulfin, S. P. Panjaitan, H. H. Rangkuti, and M. A. Siregar, "Implementation of Outdoor to Indoor Path Loss Model at 1.8 GHz and 2.1 GHz with a Transmitter Placed on Top of the Building," in *Proceeding - ELTICOM 2022: 6th International Conference on Electrical, Telecommunication and Computer Engineering 2022*, Medan, Indonesia: IEEE, 2022, pp. 111–116. doi: 10.1109/ELTICOM57747.2022.10037980.

[19] P. M. Sihombing, H. A. Samosir, L. T. Hutabarat, M. W. Sitopu, J. Margolang, and J. Hidayat, "Microstrip antenna design using meander line technique for communication between pilot and air traffic controller in VHF A/G Band," *2020 4th International Conference on Electrical, Telecommunication and Computer Engineering, ELTICOM 2020 - Proceedings*, pp. 111–114, 2020, doi: 10.1109/ELTICOM50775.2020.9230499.

[20] C. Banciu, A. Florea, and R. Bogdan, "Monitoring and Predicting Air Quality with IoT Devices," *Processes*, vol. 12, no. 9, p. 1961, Sep. 2024, doi: 10.3390/pr12091961.

[21] H. Tang *et al.*, "Multi-Scenario Validation and Assessment of a Particulate Matter Sensor Monitor Optimized by Machine Learning Methods," *Sensors*, vol. 24, no. 11, p. 3448, May 2024, doi: 10.3390/s24113448.

[22] J. A. Abdinoor *et al.*, "Performance of Low-Cost Air Temperature Sensors and Applied Calibration Techniques—A Systematic Review," *Atmosphere (Basel).*, vol. 16, no. 7, p. 842, Jul. 2025, doi: 10.3390/atmos16070842.

[23] M. Taştan, "Machine Learning–Based Calibration and Performance Evaluation of Low-Cost Internet of Things Air Quality Sensors," *Sensors*, vol. 25, no. 10, p. 3183, May 2025, doi: 10.3390/s25103183.

[24] P. M. Sihombing, M. Pinem, and S. I. Rezkika, "Analysis of the selection of propagation models from outside into the building at 1800 MHz and 2100 MHz," *SinkrOn*, vol. 5, no. 2, pp. 239–250, 2021, doi: 10.33395/sinkron.v5i2.10871.

[25] W. Gao, W. Liu, F. Li, and Y. Hu, "Analysis and Validation of Ultrasonic Probes in Liquid Level Monitoring Systems," *Sensors*, vol. 21, no. 4, p. 1320, Feb. 2021, doi: 10.3390/s21041320.

[26] S. H. Cho, Y. G. Cho, H. A. Park, and A. R. Bong, "Reliability and Validity of an Ultrasonic Device for Measuring Height in Adults," *Korean J. Fam. Med.*, vol. 42, no. 5, pp. 376–381, Sep. 2021, doi: 10.4082/kjfm.20.0202.

[27] M. Masoudimoghaddam, J. Yazdi, and M. Shahsavandi, "A low-cost ultrasonic sensor for online monitoring of water levels in rivers and channels," *Flow Measurement and Instrumentation*, vol. 102, p. 102777, Mar. 2025, doi: 10.1016/j.flowmeasinst.2024.102777.

[28] DFRobot, "A02YYUW Waterproof Ultrasonic Sensor Wiki - DFRobot," Wiki DFRobot. Accessed: Jul. 23, 2025. [Online]. Available: https://wiki.dfrobot.com/_A02YYUW_Waterproof_Ultrasonic_Sensor_SKU_SEN0311

[29] S. Ullas, B. U. Maheswari, S. Ponnekant, and T. M. M. Kumar, "A three stage attention enabled stacked deep CNN-BiLSTM (ASDCBNet) model for end-to-end monitoring of wastewater treatment plant," *Appl. Water Sci.*, vol. 15, no. 8, p. 203, Aug. 2025, doi: 10.1007/s13201-025-02575-2.

[30] S. L. Mohammed, A. Al-Naji, M. M. Farjo, and J. Chahl, "Highly Accurate Water Level Measurement System Using a Microcontroller and an Ultrasonic Sensor," *IOP Conf. Ser. Mater. Sci. Eng.*, vol. 518, no. 4, p. 042025, May 2019, doi: 10.1088/1757-899X/518/4/042025.